Development of microbial-enzyme-mediated decomposition model parameters through steady-state and dynamic analyses

Gangsheng Wang,[1] Wilfred M. Post, and Melanie A. Mayes

*Climate Change Science Institute and Environmental Sciences Division, Oak Ridge National Laboratory,
Oak Ridge, Tennessee 37831-6301 USA*

Abstract. We developed a microbial-enzyme-mediated decomposition (MEND) model, based on the Michaelis-Menten kinetics, that describes the dynamics of physically defined pools of soil organic matter (SOC). These include particulate, mineral-associated, dissolved organic matter (POC, MOC, and DOC, respectively), microbial biomass, and associated exoenzymes. The ranges and/or distributions of parameters were determined by both analytical steady-state and dynamic analyses with SOC data from the literature. We used an improved multi-objective parameter sensitivity analysis (MOPSA) to identify the most important parameters for the full model: maintenance of microbial biomass, turnover and synthesis of enzymes, and carbon use efficiency (CUE). The model predicted that an increase of 2°C (baseline temperature 12°C) caused the pools of POC-cellulose, MOC, and total SOC to increase with dynamic CUE and decrease with constant CUE, as indicated by the 50% confidence intervals. Regardless of dynamic or constant CUE, the changes in pool size of POC, MOC, and total SOC varied from −8% to 8% under +2°C. The scenario analysis using a single parameter set indicates that higher temperature with dynamic CUE might result in greater net increases in both POC-cellulose and MOC pools. Different dynamics of various SOC pools reflected the catalytic functions of specific enzymes targeting specific substrates and the interactions between microbes, enzymes, and SOC. With the feasible parameter values estimated in this study, models incorporating fundamental principles of microbial-enzyme dynamics can lead to simulation results qualitatively different from traditional models with fast/slow/passive pools.

Key words: decomposition; microbial biomass; multi-objective parameter sensitivity analysis (MOPSA); parameterization; soil enzymes.

INTRODUCTION

Recent developments in modeling of soil organic carbon (SOC) decomposition have explicitly taken into account the role of microbes as decomposers (Schimel and Weintraub 2003, Moorhead and Sinsabaugh 2006, Lawrence et al. 2009, Allison et al. 2010). Particularly, these models separate extracellular enzymes from the microbial biomass pool and directly couple the kinetics of enzymes to SOC turnover. Schimel and Weintraub (2003) incorporated an enzyme pool into a first-order or a reverse Michaelis-Menten (RM-M-SW) kinetics for SOC decomposition. Moorhead and Sinsabaugh (2006) divided the microbial community for litter decomposition into three guilds: opportunists, decomposers, and miners, which are responsible for degradation of soluble substrates, holocelluloses, and lignins, respectively. This guild-based model considered the lignocellulose index (LCI) as a key factor controlling the interactions between lignin and cellulose. The RM-M-SW was used by Lawrence et al. (2009) in an enzyme-catalyzed model

including both sorption and desorption processes. Allison et al. (2010) developed a microbial-enzyme model with the Michaelis-Menten (M-M) kinetics to simulate the responses of SOC to an increase of 5°C from 20°C using a single SOC pool.

These efforts were effective attempts to add microbial-enzyme mechanisms to traditional SOC decomposition models. However, several important issues remain to be addressed and further studied:

1) Representation of carbon pools. A single SOC pool or traditional fast/slow/passive pools are often used in SOC decomposition models. Traditional fast/slow/passive pools based on decay rates are empirical and difficult to relate to measurements (Schmidt et al. 2011). Although physically defined SOC fractions have been employed to study SOC dynamics (Six et al. 2001), they have not been considered in SOC decomposition models. Generally, the organic material in the mineral soil can be separated into particulate organic matter (POC) and mineral-associated organic matter (MOC; Schlesinger and Lichter 2001). POC, derived from plants, is defined as the organic matter carbon associated with sand-sized particles (e.g., particle size >53 μm), while MOC refers to the fraction with particle size

<53 μm (Aoyama et al. 1999, Mrabet et al. 2001, Schlesinger and Lichter 2001, Mendham et al. 2004). POC corresponds to the available SOC in Schimel and Weintraub (2003), and MOC is the physiochemically protected SOC in Conant et al. (2011). Turnover of POC can be orders of magnitude faster than those for MOC (Conant et al. 2011).

2) Representation of enzyme kinetics in models. Since SOC is largely decomposed as a result of exoenzymes produced by microorganisms, explicit representation of enzyme kinetics is an important advance in the process description of SOC dynamics. Several models used the RM-M-SW equation to simulate SOC decomposition, which relies on the concentration of enzymes rather than the concentration of substrates. Unlike the original M-M equation derived from a solid theoretical basis for a simple enzyme and a single substrate (Park and Agmon 2008), the RM-M-SW is functionally analogous to the Langmuir adsorption equation (Schimel and Weintraub 2003). However, almost no estimates of the half-saturation constant for enzyme pools in the RM-M-SW have been reported (Moorhead and Sinsabaugh 2006, Lawrence et al. 2009). Thus it is more difficult to parameterize a RM-M-SW model than a M-M model. Even for the M-M kinetics, very few estimates of the maximum specific reaction rate and the half-saturation constant for substrates have been presented outside of the aquatic literature (Moorhead and Sinsabaugh 2006).

3) Adsorption and desorption of dissolved organic carbon (DOC). The transformation of DOC is one of the rate-limiting steps in decomposition and respiration (Conant et al. 2011). In addition, DOC availability, especially in deeper soil, is controlled by sorption processes (Michalzik et al. 2003). Equilibrium sorption models (e.g., Langmuir isotherm) have been widely used to describe the adsorption/desorption processes (Kaiser and Guggenberger 2000, Hinz 2001, Kaiser et al. 2001, Neff and Asner 2001, Jardine et al. 2006, Kleber et al. 2007, Vandenbruwane et al. 2007, Mehdi et al. 2009). However, equilibrium models are not enough to account for the role of mineral-organic interactions in stabilizing SOC, since they assume that exchange between the adsorbed and dissolved phases equilibrates rapidly (Yurova et al. 2008). Actually, a 24-hour duration has been widely used in the laboratory sorption experiments (Lilienfein et al. 2004, Kothawala et al. 2008). In addition, the utilization of equilibrium models means that only net adsorption occurs even at low DOC concentration and would result in continuous augmentation of adsorbed C, which is inconsistent with the existence of a maximum sorption capacity denoted by Q_{max} (Kothawala et al. 2008, Mayes et al. 2012). Only one model includes both adsorption and desorption (Lawrence et al. 2009), where the adsorption and desorption depend on DOC concentration and slow pool size, respectively. However, the slow pool size in their model was far greater than Q_{max}. Additionally, the adsorption only depends on the concentration of DOC

in their model (Neff and Asner 2001) and disregards the amount of mineral surface available for adsorption (Sohn and Kim 2005).

4) Microbial growth and maintenance. Both growth and maintenance respiration were included in two models, with maintenance respiration proportional to microbial biomass carbon (MBC; Schimel and Weintraub 2003, Lawrence et al. 2009). Wang and Post (2012) conducted a theoretical reassessment of microbial maintenance and proposed a new model scheme to quantify growth respiration rate, maintenance respiration rate, enzyme production rate, plus microbial mortality rate, where the maintenance respiration was considered to depend on both DOC and MBC. This representation of microbial maintenance respiration is adopted in MEND developed here.

5) Model parameterization. One reason that various mechanistic processes have not been integrated into current SOC models is data unavailability (Schmidt et al. 2011). In the previous models, many parameter values were simply assumed by the researchers. Particularly, very few estimates for the kinetic parameters in the M-M equation and the adsorption/desorption rates have been documented for use in models. In addition, model development also requires determination of the relative importance of each parameter for model performance in order to evaluate the adequacy of the model parameter estimates (Wang et al. 2009, Schmidt et al. 2011).

In this study, we developed a microbial-enzyme-mediated SOC decomposition model by considering the aforementioned issues and estimated parameter values through both analytical steady-state and dynamic analyses. Using the estimated parameter ranges/distributions, we implemented a multi-objective parameter sensitivity analysis (MOPSA) to identify important parameters and investigated the effects of temperature on SOC dynamics.

METHODS

Model description

Carbon pools and fluxes in the proposed microbial-enzyme-mediated decomposition (MEND) model are shown in Fig. 1. Six carbon pools are considered in MEND: (1) particulate organic carbon (POC, represented by the variable P in model equations, see Table 1), (2) mineral-associated organic carbon (MOC, M), (3) active layer of MOC interacting with dissolved organic carbon through adsorption and desorption (Q), (4) dissolved organic carbon (DOC, D), (5) microbial biomass carbon (MBC, B), and (6) extracellular enzymes (EP and EM). The component fluxes are (1) DOC uptake by microbes (denoted by the flux F_1), (2) POC decomposition (F_2), (3) MOC decomposition (F_3), (4, 5) microbial growth respiration (F_4) and maintenance respiration (F_5), (6, 7) adsorption (F_6) and desorption (F_7), (8) microbial mortality (F_8), (9) enzyme
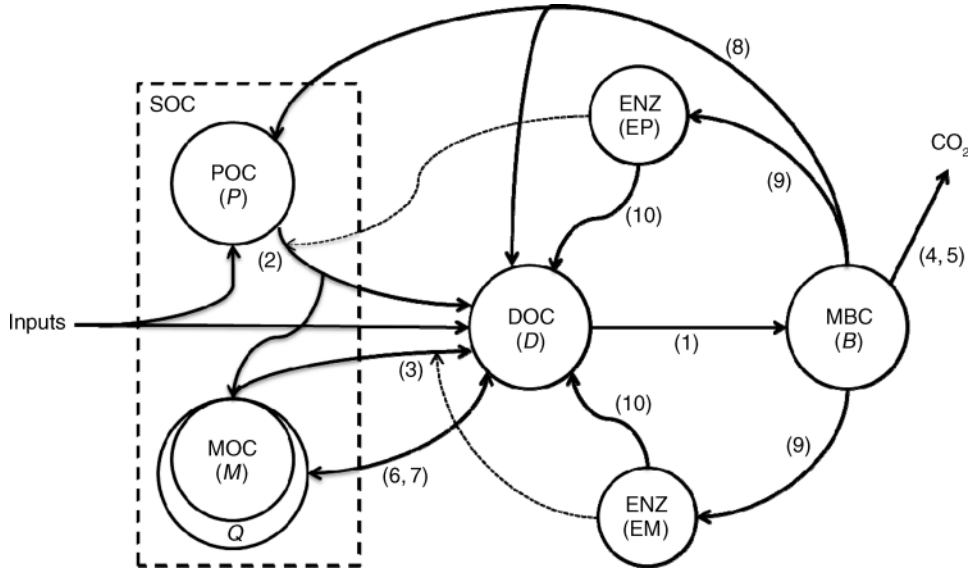
Fig. 1. Carbon pools and fluxes in the soil organic carbon (SOC) decomposition model. Circles represent carbon pools, and solid arrows represent C fluxes. Dashed arrows indicate the catalysis of SOC decompositions by extracellular enzymes. SOC has two components: particulate organic carbon (POC, P) and mineral associated organic carbon (MOC, M). Transformation processes include (1) dissolved organic carbon (DOC, D) uptake by microbial biomass (MBC, B), (2) POC pool decomposition, (3) MOC pool decomposition, (4, 5) microbial growth and maintenance respirations, (6, 7) adsorption and desorption between DOC and Q pools (the adsorbed phase of DOC interacting with DOC through adsorption and desorption), (8) microbial biomass mortality, (9) production of enzymes for decomposition of POC (EP) and MOC (EM), and (10) enzyme turnover.

production (F_9), and (10) enzyme turnover (F_{10}). Model equations for each compartment are listed as follows:

$$\frac{dP}{dt} = I_P + (1 - g_D)F_8 - F_2 \tag{1}$$

$$\frac{dM}{dt} = (1 - f_D)F_2 - F_3 \tag{2}$$

$$\frac{dQ}{dt} = F_6 - F_7 \tag{3}$$

$$\frac{dB}{dt} = F_1 - (F_4 + F_5) - F_8 - (F_{9,\text{EP}} + F_{9,\text{EM}}) \tag{4}$$

$$\frac{dD}{dt} = I_D + f_D \cdot F_2 + g_D \cdot F_8 + F_3$$
$$\quad + (F_{10,\text{EP}} + F_{10,\text{EM}}) - F_1 - (F_6 - F_7) \tag{5}$$

$$\frac{d\text{EP}}{dt} = F_{9,\text{EP}} - F_{10,\text{EP}} \tag{6}$$

$$\frac{d\text{EM}}{dt} = F_{9,\text{EM}} - F_{10,\text{EM}} \tag{7}$$

$$\frac{d}{dt}(P + M + Q + B + D + \text{EP} + \text{EM})$$
$$= I_P + I_D - (F_4 + F_5) \tag{8}$$

where F_i ($i = 1, 2, \ldots, 10$) denotes the component C fluxes,

$$F_1 = \frac{1}{E_C}(V_D + m_R)\frac{D \times B}{K_D + D} \tag{9}$$

$$F_2 = \frac{V_P \times \text{EP} \times P}{K_P + P} \tag{10}$$

$$F_3 = \frac{V_M \times \text{EM} \times M}{K_M + M} \tag{11}$$

$$F_4 = \left(\frac{1}{E_C} - 1\right)\frac{V_D \times B \times D}{K_D + D} \tag{12}$$

$$F_5 = \left(\frac{1}{E_C} - 1\right)\frac{m_R \times B \times D}{K_D + D} \tag{13}$$

TABLE 1. State variables of the model.

Variable	Description	Initial size for spin-up (mg C/g soil)
B	Microbial biomass carbon (MBC)	2
D	Dissolved organic carbon (DOC)	1
P	Particulate organic carbon (POC)	10
Q	Adsorbed phase of DOC	0.1
M	Mineral associated organic carbon (MOC) excluding Q	5
EP	Enzyme for decomposition of P	10^{-5}
EM	Enzyme for decomposition of M	10^{-5}
CO_2	Accumulated CO_2 flux	

GANGSHENG WANG ET AL.

TABLE 2. Model parameters and inputs.

Parameter	Description	Units
V_P	maximum specific decomposition rate for P by EP	mg C·mg C^{-1}·h^{-1}
K_P	half-saturation constant for decomposition of P	mg C/g soil
V_M	maximum specific decomposition rate for M by EM	mg C·mg C^{-1}·h^{-1}
K_M	half-saturation constant for decomposition of M	mg C/g soil
V_D	maximum specific uptake rate of D for growth of B	mg C·mg C^{-1}·h^{-1}
K_D	half-saturation constant of uptake of D for growth of B	mg C/g soil
m_R	specific maintenance factor or rate	mg C·mg C^{-1}·h^{-1}
E_C	carbon use efficiency	
f_D	fraction of decomposed P allocated to D	
g_D	fraction of dead B allocated to D	
p_{EP}	fraction of m_R for production of EP	
p_{EM}	fraction of m_R for production of EM	
r_{EP}	turnover rate of EP	mg C·mg C^{-1}·h^{-1}
r_{EM}	turnover rate of EM	mg C·mg C^{-1}·h^{-1}
Q_{max}	maximum DOC sorption capacity	mg C/g soil
K_{ads}	specific adsorption rate	mg C·mg C^{-1}·h^{-1}
K_{des}	desorption rate	mg C·mg C^{-1}·h^{-1}
K_{BA}	binding affinity	(mg C/g soil)$^{-1}$
I_P	input rate of P	mg C·g soil^{-1}·h^{-1}
I_D	input rate of D	mg C·g soil^{-1}·h^{-1}
fI_D	ratio of I_D to I_P	—

$$F_6 = K_{ads}\left(1 - \frac{Q}{Q_{max}}\right)D \qquad (14)$$

$$F_7 = K_{des} \times \frac{Q}{Q_{max}} \qquad (15)$$

$$F_8 = (1 - p_{EP} - p_{EM})m_R \times B \qquad (16)$$

$$F_{9,EP} = p_{EP} \times m_R \times B, \text{ and } F_{9,EM} = p_{EM} \times m_R \times B \qquad (17)$$

$$F_{10,EP} = r_{EP} \times EP, \text{ and } F_{10,EM} = r_{EM} \times EM \qquad (18)$$

where the state variables (C pools, i.e., B, D, P, Q, M, EP, and EM) and model parameters/inputs (e.g., V_P, K_P, I_P, I_D, V_D, K_D, V_M, K_M, E_C, m_R, g_D, f_D, K_{ads}, K_{des}, p_{EM}, p_{EP}) are summarized in Table 1 and Table 2, respectively. Eq. 8 expresses the overall mass balance of the full system.

The POC and DOC pools receive external inputs such as litter decomposition, plant roots, and root exudates (Kuzyakov and Domanski 2000). The decomposition processes of POC and MOC are mediated by responsible enzymes (EP and EM), respectively. A fraction (f_D) of decomposed POC enters the DOC pool and the rest ($1 - f_D$) goes to MOC. Decomposed MOC becomes another source for DOC. A pool (Q) is differentiated from MOC and defined as the adsorbed phase of DOC interacting with DOC through adsorption and desorption. The potential size of the Q pool is quantified by the maximum adsorption capacity (Q_{max}) (Kothawala et al. 2008). We assumed that the mutual conversion between MOC and Q could be neglected. The adsorption and desorption of DOC are simultaneously considered as dynamic processes in the model. The adsorption is controlled by DOC concentration and mineral surface coverage, and the desorption is pre-

sumed to only depend on surface coverage (Rudzinski and Panczyk 2000, Sohn and Kim 2005). Relative saturation of the Q pool (Q/Q_{max}, ratio of actual adsorbed C content to Q_{max}) is defined to represent the fraction of the mineral surface area occupied.

Both growth and maintenance respirations (Pirt 1965, van Iersel and Seymour 2000, Jin and Bethke 2003, van Bodegom 2007) are included in the model. The uptake of DOC by MBC, and the growth, maintenance, and turnover of MBC, follow the model scheme described by Wang and Post (2012). Small portions (p_{EP} and p_{EM}) of the physiological maintenance of MBC (quantified by the factor m_R) are allocated to enzyme production, and the turnover of MBC enters DOC with a fraction of g_D and POC with the rest of the fraction of ($1 - g_D$).

In this paper, DOC is considered as potential DOC, passing a filter pore size of 0.4–0.6 μm (Novak et al. 1992, Kalbitz et al. 2000, Chantigny 2003), that contains organic carbon from the decomposition of POC and MOC, the desorption of C from mineral surfaces, enzymes, and the death of MBC. It is similar to the concept of "available DOC" postulated by Schimel and Weintraub (2003) and "soluble organic carbon" used by Qualls (2000). Therefore, the DOC used in our model includes DOC present in soil solution and potentially soluble organic carbon, but in solid state.

Model parameterization

Data for SOC, DOC, and MBC, and related climate, soil, and land use conditions were collected from 985 observations in 177 publications (see full data in the Supplement). Generally, the depth of these soil samples ranged from 0.1 to 0.5 m with an average depth of 0.25 m. In addition, values for some parameters (e.g., K_D, m_R, E_C, Q_{max}, binding affinity [K_{BA}]) and external inputs ($I = I_P + I_D$) were also summarized through literature research (Wang et al. 2012b). Based on these

data and the steady-state solutions, values or ranges for the other model parameters could be estimated. From the analysis of Wang and Post (2012), the values of specific maintenance rate, maintenance coefficient, and turnover rate of MBC were combined to quantify the specific maintenance factor (m_R). Literature values of K_{BA} are expressed in units of (mg C/L solution)$^{-1}$ because it is usually derived from sorption experiments using soil solutions. We converted K_{BA} to values in units of (mg C/g soil)$^{-1}$ by presuming that the dimensionless quantities, $D_{eq}K_{BA}$ (D_{eq} is the equilibrium concentration of DOC), are equivalent under different unit systems.

Statistical analysis of literature data was conducted using R software (R Development Core Team 2011). The Kolmogorov-Smirnov goodness-of-fit (KS) test was adopted for the normality test (software *available online*).[2] The significance of difference between categorical data was tested by the non-parametric Kruskal-Wallis (KW) test (see footnote 2; Ott and Longnecker 2010). Both KS and KW tests were conducted at a significance level of 0.05.

<center>*Multi-objective parameter sensitivity analysis*</center>

The parametric sensitivity analysis is important for model parameterization (Wang and Chen 2012, Wang et al. 2012*a*). Based on the estimated parameter ranges, we could identify the critical parameters for the dynamics of each pool through an improved multi-objective parameter sensitivity analysis (MOPSA). The original MOPSA in Wang and Chen (2012) was developed based on the multi-parameter sensitivity analysis (MPSA) algorithm, which is a global sensitivity analysis method (Rodrigue-Fernandez et al. 2012). The consideration of multiple objectives is essential in models with many processes and state variables (Wang and Xia 2010). We used this improved MOPSA approach to increase our ability to quantitatively interpret the results over previous MOPSA in Wang and Chen (2012). The improved MOPSA consists of the following steps:

1) Select the parameters to be evaluated and generate parameter sets in terms of their distributions and ranges based on the parameterization process described in the previous section.

2) Run the model with these parameter sets and compute the objective function values (OBFs) in terms of a specific response variable. The OBFs are defined as the sum of squared errors between observed and simulated time-series data. In particular, observed values achieve the OBF using the medians of parameters.

3) Identify whether the parameter sets are acceptable or unacceptable by comparing the OBFs to a given criterion, e.g., the 50% divisions of the sorted OBFs (Choi et al. 1998). The OBF less than the criterion is

[2] http://cran.r-project.org/web/packages/pgirmess/index.html

classified as acceptable, otherwise it is classified as unacceptable.

4) For the *i*th parameter, if it follows a log-transformed distribution (e.g., log-normal or log-uniform has been used in step 1), let $X_i = \{x_{i,j}, j = 1, 2, \ldots, 2n\}$ be the logarithmic parameter values; otherwise, let X_i be the original values. Define $x_{i,\min} = \min\{X_i\}$ and $x_{i,\max} = \max\{X_i\}$, and the normalized X_i, denoted by $Xn_i = \{xn_{i,j}, j = 1, 2, \ldots, 2n\}$, is defined as

$$xn_{i,j} = \frac{x_{i,j} - x_{i,\min}}{x_{i,\max} - x_{i,\min}} \in [0, 1]. \quad (19)$$

5) Let $Xn_i^A = \{xn_{i,j}^A, j = 1, 2, \ldots, n\}$ and $Xn_i^U = \{xn_{i,j}^U, j = 1, 2, \ldots, n\}$ be the sorted (in ascending order) subsets of acceptable (A) and unacceptable (U) Xn_i, respectively. Plot the cumulative probability distribution (CPD) curves for the acceptable and unacceptable subsets. Compute the average "discrepancy" between the two CPD curves as the sensitivity index (SI):

$$SI_i^k = \frac{1}{n} \sum_{j=1}^{n} \left| xn_{i,j}^A - xn_{i,j}^U \right| \quad (20)$$

where SI_i^k is the sensitivity index of the *i*th parameter for the *k*th response variable.

6) Evaluate the sensitivity of each parameter by the sensitivity plots and the SI values. The sensitivity plot qualitatively shows the discrepancy between the two CPD curves. In addition, the SI value quantitatively describes the relative sensitivity between parameters. A large difference means that the response variable is highly sensitive to the changes in that parameter. Similarly, a higher SI value implies a higher sensitivity of the parameter.

7) The above analysis is conducted for a single objective (i.e., a single response variable). The overall parameter sensitivity index of a model with multiple response variables can be estimated as

$$SI_i = \frac{1}{m} \sum_{k=1}^{m} SI_i^k \quad (21)$$

where SI_i denotes the overall sensitivity index for the *i*th parameter in terms of *m* response variables.

Log-normalization is required for those parameters with log-transformed distributions in step 4 to make the sensitivity plots and the SI values comparable among parameters. The sensitivity index used here is a relative concept. The SI values can be used to compare the sensitivities between different parameters pertaining to a specific objective function or an integrated function of multi-objective. A parameter with higher SI value is more sensitive (or important) than another parameter with lower SI value.

<center>*SOC responses to warming: model application*</center>

The SOC dynamics is influenced by environmental factors, especially temperature (Davidson and Janssens

TABLE 3. Activation energies (Ea) for selected parameters.

Parameter	Activation energy (kJ/mol)	Reference
V_P, lignin	53 ± 17	Wang et al. (2012b)
V_P, cellulose	37 ± 15	Wang et al. (2012b)
V_M, V_D	47	Allison et al. (2010)
K_P, K_M, K_D	30	Davidson et al. (2006)
m_R	20	van Iersel and Seymour (2002)
K_{ads}	5	Elshafei et al. (2009)
K_{des}	20	Kaiser et al. (2001)

Note: Activation energy values for V_P are means ± SD.

2006). However, the impacts of warming on SOC dynamics are uncertain (Conant et al. 2011). We provided an analysis of our model formulation to hypothetical temperature changes. For this we require additional model development, consistent with our enzyme kinetic formulation. Since POC receives plant-derived materials as inputs (McGuire and Treseder 2010), we assumed that the POC pool consists of two substrates (lignin and cellulose/hemicellulose). Each substrate has associated enzymes that convert it into dissolved monomers (DOC). Lignin is decomposed by oxidative enzymes (ligninases) produced by appropriate microbes (fungi), and cellulose/hemicellulose is decomposed with hydrolytic enzymes (cellulases) produced by bacteria and fungi (Wang et al. 2012b). The allocation of EP production to ligninase and cellulase was presumed to be proportional to the corresponding substrate pool size. We investigated the SOC pools changing with time under warming conditions by conducting numerical simulations.

The Arrhenius equation was used to simulate the response of parameter values to changes in temperature (Wang et al. 2012b):

$$V(T) = V(T_{ref})\exp\left[-\frac{Ea}{R}\left(\frac{1}{T} - \frac{1}{T_{ref}}\right)\right] \quad (22)$$

where $V(T)$ and $V(T_{ref})$ are the parameter values at the temperature T (K) and the reference temperature T_{ref} (K), respectively; Ea is the energy of activation (kJ/mol); and $R = 8.314$ J·mol^{-1}·K^{-1}, is the universal gas constant.

The activation energy (Ea) in the Arrhenius equation for selected parameters is shown in Table 3. The specific reaction rate for lignin degradation had a higher Ea than that of cellulose (Wang et al. 2012b). Ea for the half-saturation constants (K_P, K_M, and K_D) was set as 30 kJ/mol, corresponding to a Q_{10} of 1.5 for temperature ranging 20–30°C (Davidson et al. 2006). The microbial maintenance is also dependent on temperature (van Iersel and Seymour 2002). Elshafei et al. (2009) observed a low Ea, i.e., 4.36 and 5.04 kJ/mol for DOC adsorption in clay and sandy soils, which was consistent with the observations of no apparent effect of temperature on it (Kaiser et al. 2001, Mehdi et al. 2009). As shown in Table 3, Ea for adsorption is smaller than that for desorption (Conant et al. 2011). The temperature-modification of carbon use efficiency (CUE, denoted by E_C in equations) is described by a linear function:

$$E_C(T) = E_C(T_{ref}) - k_{EC}(T - T_{ref}) \quad (23)$$

where $0 < E_C(T) < 1$ in this study and the slope k_{EC} was set to 0.012°C^{-1} (Devevre and Horwath 2000).

The baseline soil temperature and pH value were set as 12°C and 6, respectively. The baseline temperature of 12°C is close to the mean annual temperature of 11.6°C for the United States (NOAA 2011). The baseline pH of 6 is the mean soil pH value calculated from literature data (see Table 4).

We simulated the responses of C pool sizes to a temperature increase of 2°C against the control treatment (12°C) by sampling the parameters from their respective distributions/ranges. Only those parameter sets that could result in a feasible steady-state system were used for further analysis. The steady-state C pool sizes were then adopted as initial values for scenario analysis over a 100-yr period. The values of parameters shown in Table 3

TABLE 4. Summary of soil organic carbon data from the literature (the associated full data are presented in the Supplement).

Soil order	SOC		DOC		MBC		pH	
	n	$\log_{10}(SOC)$	n	$\log_{10}(DOC)$	n	$\log_{10}(MBC)$	n	pH
Alfisols	154	$1.19^{cd} \pm 0.30$	18	$-0.79^b \pm 0.56$	25	$-0.33^b \pm 0.41$	141	$6.3^{bc} \pm 0.7$
Andisols	52	$1.77^b \pm 0.21$	34	$-0.64^b \pm 0.50$	28	$-0.60^b \pm 0.45$	45	$5.8^{cd} \pm 0.9$
Aridisols	23	$0.92^d \pm 0.39$	4	$-0.96^b \pm 0.26$	1	-0.45	21	$7.6^a \pm 0.4$
Entisols	81	$0.94^d \pm 0.54$	17	$-1.56^b \pm 0.52$	14	$-0.44^{ab} \pm 0.72$	61	$6.3^{bcd} \pm 1.2$
Gelisols	49	$1.77^b \pm 0.63$	21	$-0.51^b \pm 0.42$	7	$0.58^a \pm 0.69$	28	$5.4^{de} \pm 1.2$
Histosols	44	$2.38^a \pm 0.23$	5	$0.01^a \pm 0.35$	7	$0.23^a \pm 0.24$	21	$5.5^{de} \pm 1.2$
Inceptisols	204	$1.43^b \pm 0.48$	47	$-0.86^b \pm 0.41$	62	$-0.12^{ab} \pm 0.32$	169	$5.8^d \pm 1.2$
Mollisols	88	$1.33^c \pm 0.31$	9	$-0.64^b \pm 0.44$	11	$-0.18^{ab} \pm 0.31$	75	$7.0^a \pm 1.0$
Oxisols	24	$1.41^{bc} \pm 0.36$	7	$-1.19^b \pm 0.85$	19	$-0.34^b \pm 0.49$	21	$5.6^{de} \pm 0.8$
Spodosols	62	$1.61^b \pm 0.53$	20	$-0.92^b \pm 0.50$	14	$-0.08^{ab} \pm 0.47$	56	$4.7^e \pm 0.9$
Ultisols	117	$1.15^c \pm 0.46$	14	$-1.08^b \pm 0.41$	75	$-0.42^b \pm 0.43$	109	$5.7^d \pm 1.0$
Vertisols	18	$1.17^{cd} \pm 0.39$	3	$-1.56^b \pm 0.30$	12	$-0.36^b \pm 0.24$	16	$7.3^a \pm 0.8$
All	916	1.38 ± 0.54	199	-0.85 ± 0.56	275	-0.29 ± 0.48	763	6.0 ± 1.2

Notes: Values are mean ± SD of log-transformed soil organic carbon (SOC), dissolved organic carbon (DOC), or microbial biomass carbon (MBC), measured as mg C/g soil; n is the number of observations. Different superscript letters after means indicate significantly different means according to the Kruskal-Wallis (KW) test at $\alpha = 0.05$.
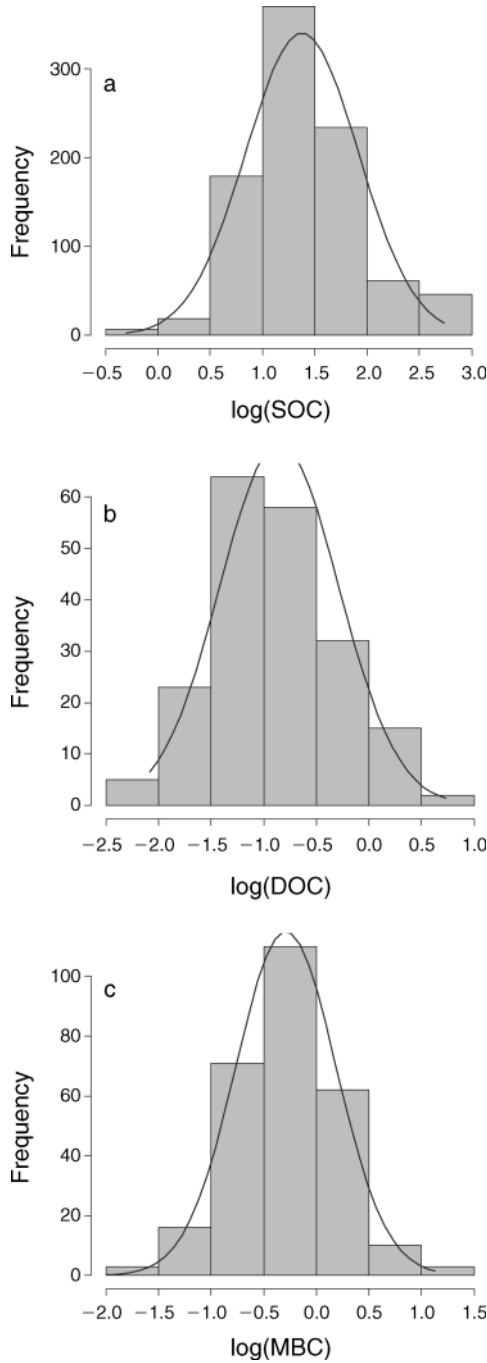
FIG. 2. Histogram of log-transformed (a) soil organic carbon (SOC), (b) dissolved organic carbon (DOC), and (c) microbial biomass carbon (MBC), all measured as mg C/g soil.

were modified by temperature changes. Two scenarios were examined: dynamic CUE, with CUE changing with temperature as described by Eq. 23, and constant CUE, with the same CUE as the control treatment.

We also investigated the temporal evolutions of C pool sizes by conducting model simulations to a hypothetical step-wise temperature change using a single

parameter set. The typical parameter values estimated in model parameterization were adopted in this case. The V_P values ($T = 12°C$ and pH = 6) for POC-lignin and POC-cellulose were set to 0.96 and 5.02 mg C·mg $C^{-1}·h^{-1}$, respectively (Wang et al. 2012b). Five scenarios of 1–5°C temperature increase with the parameters showing in Table 3 and CUE changing with temperature were considered. A sixth scenario of 2°C temperature increase with the same CUE (0.47) as the control treatment was also included to compare with the results from the first five scenarios.

RESULTS AND DISCUSSION

Summary of pool sizes from the literature

The KS normality tests on SOC, DOC, and MBC indicated that none of them followed a normal distribution ($P < 1 \times 10^{-10}$). Both $\log_{10}(DOC)$ and $\log_{10}(MBC)$ were normally distributed ($P = 0.37$ and 0.71, respectively). Although $\log_{10}(SOC)$ was not strictly normally distributed ($P = 3 \times 10^{-4}$), we computed the mean and standard deviation (SD) from $\log_{10}(SOC)$ rather than directly from SOC. Histograms for log-transformed SOC, DOC, and MBC are shown in Fig. 2. Statistics for these data as well as soil pH values classified by soil orders are summarized in Table 4. The soil pH values can be used to modify the decomposition rates through an exponential-quadratic function as described in Wang et al. (2012b). Considering an average soil depth of 0.25 m and bulk density of 1 g/cm^3, the back-transformed mean SOC is equivalent to 6 kg C/m^2, which is close to the SOC density for cultivated land (7.9 kg C/m^2) derived by Post et al. (1982). The enzyme concentration in soils was estimated as 1×10^{-5} to 5×10^{-3} mg C/g soil (Tabatabai 2003).

Analytical steady-state solutions

Under steady state conditions, the C pools can be analytically determined from Eqs. 1–7 as follows:

$$P_{eq} = \frac{K_P}{V_P \frac{p_{EP}}{r_{EP}} \frac{E_C}{A}\left(\frac{I_D}{I_P}+1\right) - 1} \approx \frac{K_P}{\frac{V_P \times p_{EP}}{r_{EP}} \frac{E_C}{1 - g_D E_C} - 1} \tag{24}$$

$$M_{eq} = \frac{K_M}{V_M \frac{p_{EM}}{r_{EM}} \frac{E_C}{(1-f_D)A}\left(1 + \frac{I_D}{I_P}\right) - 1}$$

$$\approx \frac{K_M}{\frac{V_M \times p_{EM}}{r_{EM}} \frac{E_C}{(1 - g_D E_C)(1-f_D)} - 1} \tag{25}$$

$$Q_{eq} = \frac{Q_{max}}{1 + V_D/(m_R K_D K_{BA})} = \frac{Q_{max}}{1 + 1/(D_{eq}K_{BA})} \tag{26}$$

$$B_{eq} = \frac{I_D + I_P}{(1/E_C - 1) \times m_R} \tag{27}$$

TABLE 5. Model parameterization.

Parameter	Values†	Typical value	Reference
$I = I_D + I_P$	$\log_{10}(I) = -3.8 \pm 0.3$	1.6×10^{-4}	Wang et al. (2012b)
m_R	$\log_{10}(m_R) = -3.6 \pm 0.7$	2.8×10^{-4}	this study
E_C	$0.609-0.012T$ (°C)	0.47	Devevre and Horwath (2000)
f_D, g_D	0.5 [0.2–0.8]	0.5	Hunt (1977), this study
r_{EP}, r_{EM}	$\log_{10}(r_{EP}) = -3.0 \pm 0.5$	1×10^{-3}	Allison et al. (2010), this study
p_{EP}, p_{EM}	$\log_{10}(p_{EP}) = -2.0 \pm 0.5$	1×10^{-2}	this study
Q_{max}	1.7 ± 1.1	1.7	Mayes et al. (2012)
K_{BA}	6 ± 5	6	this study
K_{des}	1×10^{-3} [10^{-4}–10^{-2}]	1×10^{-3}	this study
K_{ads}	$K_{BA} \times K_{des}$	6×10^{-3}	this study
K_D	0.26 ± 0.12	0.26	van de Werf and Verstraete (1987)
V_D	$\log_{10}(V_D) = -3.3 \pm 0.7$	5×10^{-4}	this study
V_P	0.2–33.0	2.5	this study
K_P	$P_{eq}(a_P \times V_P - 1)$, $a_P = 6$ [3–11]	50	this study
V_M	0.05–22.0	1	this study
K_M	$M_{eq}(a_M \times V_M - 1)$, $a_M = 14$ [4–51]	250	this study

Notes: See Table 2 for description of parameters; I denotes the model inputs.
† Values shown are means; error is SD, ranges in brackets are lower bound and upper bound.

$$D_{eq} = \frac{K_D}{V_D/m_R} \qquad (28)$$

$$EP_{eq} = B_{eq} \times \frac{m_R p_{EP}}{r_{EP}} \qquad (29)$$

$$EM_{eq} = B_{eq} \times \frac{m_R p_{EM}}{r_{EM}} \qquad (30)$$

where $A = 1 - E$

$_C + (1 - p_{EP} - p_{EM}) \times E_C(1 - g_D)(I_D/I_P + 1)$; under the condition of input of DOC/input of POC $(I_D/I_P) \ll 1$ and because of $p_{EP} + p_{EM} \ll 1$, $A \approx 1 - g_D \times E_C$; the subscript eq denotes the steady state solution; and $K_{BA} = K_{ads}/K_{des}$ is the binding affinity ([mg C/g soil]$^{-1}$) as defined in the Langmuir isotherm (Kothawala et al. 2008). The assumption of $I_D/I_P \ll 1$ is based on the consideration that DOC in the mineral soil is derived from decomposed SOC and the DOC input from recent litter is limited (Michalzik et al. 2003, Fröberg et al. 2007).

Estimation of parameter values

The parameter values or probability distributions are summarized in Table 5. Some of the parameter values were collected from the literature. Both input rates ($I = I_D + I_P$) and specific maintenance factor (m_R) were log-normal distributed (see Fig. 3a and 3b, $P = 0.7$ and 0.2, respectively). The back-transformed m_R from the log-normal distribution had a mean of 2.8×10^{-4} mg C·mg C^{-1}·h^{-1} with 1 SD interval of (6.3×10^{-5}, 1.3×10^{-3}). The 1 SD interval for m_R is the back-transformed interval from the 1 SD interval of $\log_{10}(m_R)$. Values of I were converted to carbon inputs in units of mg C·g soil^{-1}·h^{-1}. The back-transformed I has an average of 1.6×10^{-4} mg C·g soil^{-1}·h^{-1} ($\log_{10}I = -3.8 \pm 0.3$) (Wang et al. 2012b). Both fraction of decomposed POC allocated to DOC (f_D) and fraction of dead MBC allocated to

DOC (g_D) were assumed to be 0.5 (Hunt 1977). The average C contents from all observations (Table 4) were used as steady-state pool sizes.

From Tabatabai (2003), the estimated enzyme concentration of α-glucosidase and β-glucosidase ranges from 1×10^{-5} to 5×10^{-3} mg C/g soil, with a mean value of 2×10^{-4} mg C/g soil, assuming that it follows a log-normal distribution. Considering that "the actual concentrations of enzyme proteins in soils are undoubtedly much greater than those calculated" (Tabatabai 2003), we adopted an enzyme concentration of 1×10^{-3} mg C/g soil, which is an order of magnitude higher than the mean value. Provided the concentration of equilibrium MBC (B_{eq}) from Table 4, specific maintenance factor (m_R) and enzyme turnover rate (r_{EP}) in Table 5, and enzyme concentration (EP_{eq}) $= 1 \times 10^{-3}$ mg C/g soil, we estimated the fraction of m_R for production of EP (p_{EP}) $\approx 1\%$ based on Eq. 29. We assumed that $p_{EM} \approx p_{EP}$.

Adapting the values for half-saturation constant of uptake of DOC for MBC growth (K_D) from Van de Werf and Verstraete (1987) and DOC concentration (D_{eq}) from Table 4, we could estimate the maximum specific uptake rate of DOC for growth of MBC (V_D) $\approx 2m_R$ by Eq. 28. For agricultural soils, turnover rates of DOC were found to be $2.5-4.2 \times 10^{-4}$ h^{-1} (Gjettermann et al. 2008), which was within the range derived in this study.

Generally, the SOC substrates were assumed to be under-saturated (Moorhead and Sinsabaugh 2006, Allison et al. 2010), which implies that the half-saturation constants K_P and K_M have the following relation with steady-state POC and MOC concentrations, respectively, $0.01 < P_{eq}/K_P < 1$ and $0.01 < M_{eq}/K_M < 1$. The lower bound of 0.01 was set for the two ratios (P_{eq}/K_P and M_{eq}/K_M) in order to make the M-M kinetics functional. Carbon use efficiency (E_C) is negatively dependent on temperature (Devevre and

Horwath 2000), and $E_C = 0.47$ at $T = 12°C$. Eqs. 24 and 25 can be rearranged as follows:

$$P_{eq}/K_P = 1/(a_P V_P - 1) \qquad (31)$$

$$M_{eq}/K_M = 1/(a_M V_M - 1) \qquad (32)$$

where $a_P = p_{EP}/r_{EP} \times E_C/(1 - g_D E_C)$ and $a_M = p_{EM}/r_{EM} \times E_C/(1 - g_D E_C)/(1 - f_D)$.

With the assumption that $p_{EP}/r_{EP} = 10$, and f_D and $g_D \in (0.2, 0.8)$, we obtained that $a_P \in (3, 11)$ and $a_M \in (4, 51)$. From Eqs. 31 and 32, we plotted P_{eq}/K_P against V_P and M_{eq}/K_M against V_M (Fig. 4). Based on the above constraints for P_{eq}/K_P and M_{eq}/K_M, we derived $V_P = 0.2–33$ (mean ≈ 2) and $V_M = 0.05–22$ (mean ≈ 1) mg C·mg C^{-1}·h^{-1}. Allison et al. (2010) set $V = 0.42$ mg C·mg C^{-1}·h^{-1} at 20°C, which fell into our parameter range. The V values from laboratory experiments with purified ligninases and cellulases had a 1 SD interval of 1×10^1 to 1×10^3 (Wang et al. 2012b), which was at least one order of magnitude higher than the V values derived here.

Jastrow (1996) measured the POC and MOC fractions in long-term cultivated soils and found that they were about 20% and 80% of the SOC contents, respectively. Under the condition of $P_{eq} + M_{eq} = 24$ mg C/g soil (Table 4), one could estimate P_{eq} and M_{eq} as 5 and 19 mg C/g soil, respectively. Using the above P_{eq} and M_{eq} and mean V_P and V_M, we calculated that $K_P = 50$ and $K_M = 250$ mg C/g soil, respectively. Similarly, if $P_{eq} + M_{eq} = 110$ as used by Allison et al. (2010), one could derive $K_P = 240$ and $K_M = 1100$, whose range contained the half-saturation constant of 500 mg C/cm^3 soil in Allison et al. (2010).

According to Mayes et al. (2012), the binding affinity $K_{BA,L}$ (subscript L denotes the value for the liquid or solution condition) was estimated as 0.06 ± 0.05 (mg C/L)$^{-1}$. In addition, DOC concentration in mineral soil of temperate forest was $D_{eq,L} = 13.8 \pm 12.1$ mg C/L (Michalzik et al. 2001). Table 4 indicated an average DOC concentration of $D_{eq} = 0.14$ mg C/g soil (1 SD interval, 0.04–0.52). We have assumed that the dimensionless quantity $(D_{eq} K_{BA})$ in Eq. 26 should be equivalent under different unit systems, i.e., $D_{eq} K_{BA} = D_{eq,L} K_{BA,L}$, which yielded $K_{BA} \approx 100 K_{BA,L} = 6 \pm 5$ (mg C/g soil)$^{-1}$.

Since the analytical steady-state solutions only depended on K_{BA}, i.e., the ratio of K_{ads} to K_{des}, dynamic analysis (numerical simulation) was conducted to determine the values of K_{ads} and K_{des}. The initial values for state variables (Table 1) and typical parameter values (Table 5, specifically $K_{des} = 1 \times 10^{-3}$) were adopted to reach a steady state. These steady-state pool sizes were then used as model initialization with K_{des} varying from 1×10^{-5} to 1 mg C·g soil^{-1}·h^{-1}. Hourly changes of Q and DOC during the first year (8760 h) are shown in Fig. 5. When K_{des} was reduced from 1×10^{-4} to 1×10^{-5}, the changes in Q and DOC were not significant compared with the others (see Fig. 5a and 5b, respectively). As $K_{des} > 0.01$, both DOC and Q departed
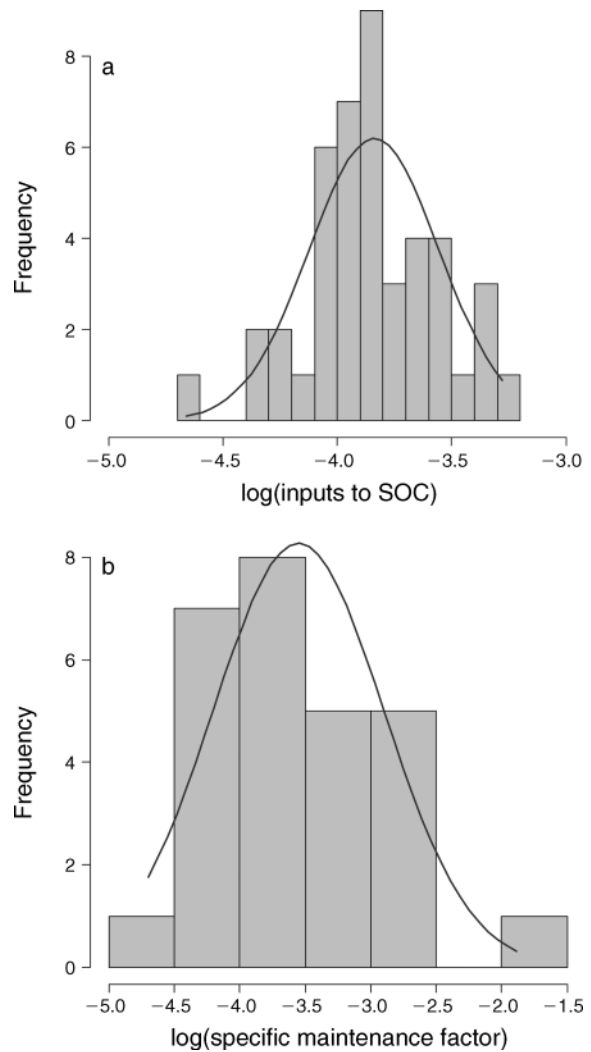

FIG. 3. Histogram of log-transformed (a) inputs to SOC (I, mg C·[g soil]$^{-1}$·h^{-1}) and (b) specific maintenance factor (m_R, mg C·[mg C]$^{-1}$·h^{-1}).

from the steady state quickly within the first day. Therefore, we estimated K_{des} as 1×10^{-4} to 1×10^{-2} mg C·g soil^{-1}·h^{-1}. The desorption rate in Lawrence et al. (2009) was close to our lower bound of K_{des}, because the slow pool in their model is analogous to but larger than the Q pool in our model.

Although we summarized the data of SOC, DOC, and MBC classified by soil orders (Table 4), we did not think there is sufficient information to separately parameterize the model with respect to soil orders. Taking the SOC as an example, there were no significant differences among Gelisols, Spodosols, Andisols, and Inceptisols according to the KW test at $\alpha = 0.05$, neither were among Oxisols, Ultisols, Mollisols, Vertisols, and Alfisols. Therefore, we only estimated the parameters for a "mean" soil type. Actually, the parameterization results shown in Table 5 are proposed general parameter ranges/distributions from considering the parameter uncertainty. In partic-
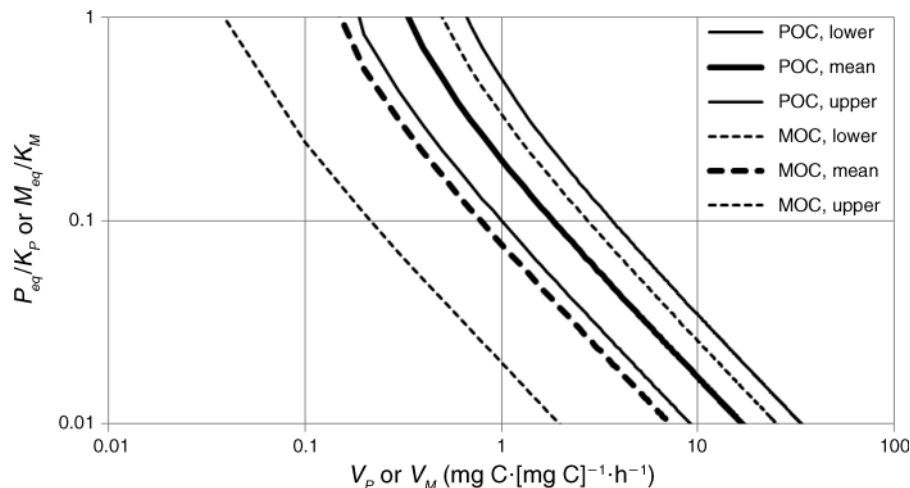
FIG. 4. Relationship between P_{eq}/K_P or M_{eq}/K_M and V_P or V_M; P_{eq} and M_{eq} are equilibrium concentrations, V_P and V_M are maximum specific decomposition rates, and K_P and K_M are half-saturation constants for particulate organic carbon (POC, P) and mineral-associated organic carbon (MOC, M), respectively. Mean, lower, and upper denote mean value and lower and upper bounds, respectively.
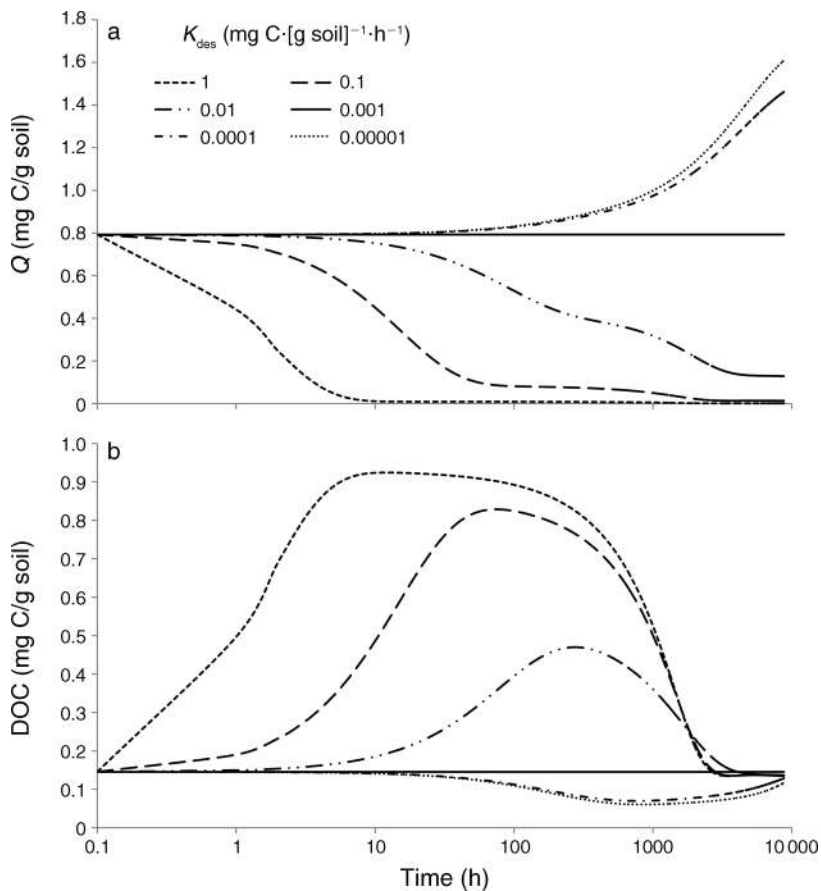

FIG. 5. Determination of desorption rate (K_{des}) with binding affinity $K_{BA} = 6$ (mg C/g soil) from dynamics of (a) adsorbed phase of DOC (Q) and (b) dissolved organic carbon (DOC).

Table 6. Parameter sensitivity analysis.

Parameter	D SI	D Order	B SI	B Order	P SI	P Order	M SI	M Order	Q SI	Q Order	EP/EM SI	EP/EM Order	CO$_2$ SI	CO$_2$ Order
m_R	0.083	16	0.087	17	0.024	10	0.011	6	0.047	16	0.053	15	0.078	17
r_{EP}	0.025	13	0.019	12	0.083	16	0.057	17	0.003	5	0.072	17	0.021	11
E_C	0.019	11	0.056	16	0.036	13	0.039	14	0.005	10	0.051	14	0.009	5
p_{EP}	0.013	9	0.018	11	0.059	14	0.039	13	0.003	4	0.059	16	0.024	12
K_P	0.006	6	0.003	2	0.143	17	0.038	12	0.002	2	0.005	3	0.013	10
V_D	0.108	17	0.003	3	0.019	8	0.011	7	0.041	15	0.011	9	0.011	9
K_M	0.031	14	0.038	15	0.006	4	0.048	16	0.003	3	0.024	12	0.056	15
fI_D	0.008	7	0.020	13	0.029	12	0.037	10	0.005	7	0.038	13	0.061	16
V_M	0.033	15	0.027	14	0.003	2	0.037	11	0.005	9	0.022	11	0.049	14
Q_{max}	0.005	5	0.008	9	0.007	6	0.004	2	0.112	17	0.008	6	0.009	6
V_P	0.011	8	0.006	5	0.077	15	0.027	8	0.005	8	0.003	1	0.003	3
I_P	0.004	1	0.014	10	0.003	3	0.039	15	0.002	1	0.013	10	0.043	13
f_D	0.018	10	0.007	7	0.022	9	0.035	9	0.012	12	0.009	7	0.003	2
K_{BA}	0.005	2	0.006	4	0.006	5	0.007	5	0.036	14	0.010	8	0.007	4
K_D	0.023	12	0.007	8	0.007	7	0.005	4	0.012	11	0.006	4	0.010	7
g_D	0.005	4	0.006	6	0.025	11	0.005	3	0.004	6	0.008	5	0.011	8
K_{des}	0.005	3	0.003	1	0.003	1	0.002	1	0.017	13	0.005	2	0.003	1

Notes: Response (state) variables are described in Table 1. For sensitivity index (SI), a greater value indicates more sensitive. Order is the ordering of sensitivity by SI, with a greater number indicating more sensitive.

ular, quantitative relationships between V and K in the M-M equations for POC and MOC decomposition were developed jointly. If there is no other data or information available, the categorized data based on soil orders could be used as a reference.

Sensitivity analysis

Based on the parameterization results shown in Table 5, the MOPSA was conducted in terms of the response variables shown in Table 1. Because we did not differentiate the parameters (enzyme production and loss rates) between EP and EM, the time evolutions of the two pools were the same. Therefore, seven response variables ($m = 7$, see Table 6) were considered in MOPSA. In addition, although we assumed the fractional input rate ($fI_D = I_D/I_P \ll 1$, and $f_D = g_D = 0.5$ in the steady-state analysis, we adopted uniform distributions for fI_D (range, 0.05–1) and f_D and g_D (range, 0.2–0.8) in MOPSA. We also assumed log-normal distributions for r_{EP} (-3.0 ± 0.5 [mean ± SD]) and p_{EP} (-2.0 ± 0.5). In summary, 17 parameters ($k = 17$) including the C input rates were considered in sensitivity analysis, and the results are shown in Table 6. For each response variable, there were two columns quantifying the sensitivity: the first column showing the SI values and the second column indicating the ordering of the sensitivity based on SI. It is evident that the relative importance of parameters depends on the response variable. For example, the most sensitive (important) parameters for the MBC pool (B) were m_R, E_C, K_M, V_M, fI_D, and r_{EP}; the most important parameters regarding POC were K_P, r_{EP}, V_P, p_{EP}, E_C, and fI_D; and the Q pool was most sensitive to changes in Q_{max}, m_R, V_D, K_{BA}, K_{des}, and f_D. Several sensitivity plots in terms of MBC are shown in Fig. 6 to illustrate the CPD curves for acceptable and unacceptable parameter values.

As shown in Fig. 7, the overall parameter sensitivity indicated that the maintenance factor of microbial biomass (m_R) was rated highest and the desorption rate (K_{des}) rated lowest among the parameters. Using the k-means clustering (Likas and Vlassis 2003), we classified the 17 parameters into five groups (G1–G5) with sensitivity from high to low: G1 (m_R), G2 (r_{EP}, E_C, p_{EP}, K_P, V_D, K_M, and fI_D), G3 (V_M and Q_{max}), G4 (V_P, I_P, and f_D), and G5 (K_{BA}, K_D, g_D, and K_{des}). The parameters within each group were considered to have similar sensitivity. The enzyme production and turnover rates (p_{EP} and r_{EP}) were as important as the CUE (E_C). Therefore, the function of enzymes in catalyzing SOC decomposition is considerable, although the enzyme concentrations are very small compared to the other C pools. As for adsorption/desorption, the maximum sorption capacity (Q_{max}) was more important than K_{BA} and K_{des}. Although K_{BA} and K_{des} fell into the same group, the SI value for K_{BA} was higher than K_{des}.

One of the main objectives of a sensitivity analysis is to evaluate the relative significance of each parameter (Choi et al. 1998, Wang and Chen 2012). The typical sensitivity analysis (SA), which investigates how an observable quantity varies with changes in the parameter, also serves this objective. The more sensitive a parameter is, the more important it is. However, the local SA is conducted in terms of single parameter in the neighborhood of a single parameter value (Van Griensven et al. 2006, Wang and Post 2012). The sensitivity index measures the average "distance" or "difference" between the two cumulative curves, not the "difference" between two means. Determining the sensitivity from the perspective of probability distribution rather than from the simple mean value is one of the advantages of MOPSA over the typical SA. Since computing a P value using the mean and standard deviation requires that a variable follows or can be
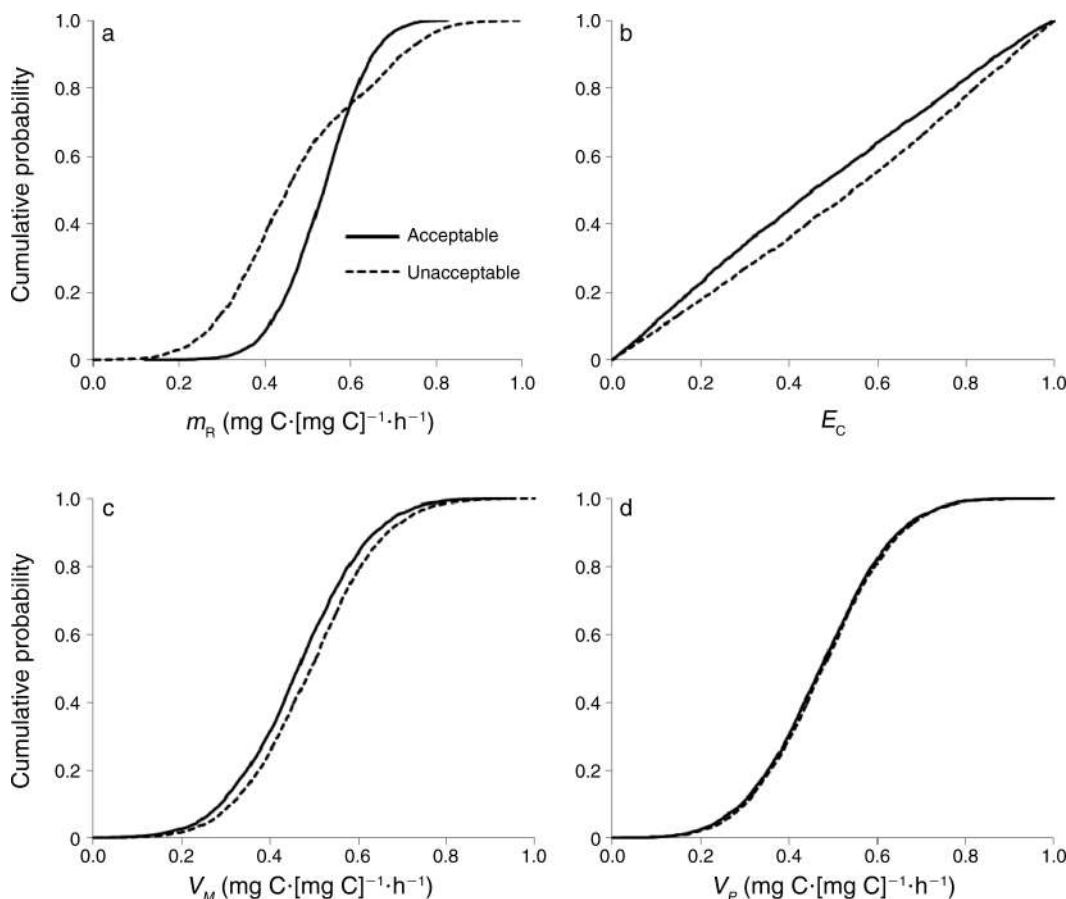
FIG. 6. Examples of cumulative probability distributions of acceptable and unacceptable parameter values by parameter sensitivity analysis; response variable: microbial biomass carbon (MBC). Parameters are (a) specific maintenance factor (m_R), (b) carbon use efficiency (E_C), and (c, d) maximum specific enzyme activity for (c) mineral-associated organic carbon (V_M) and (d) particulate organic carbon (V_P).

transformed to a normal distribution, which is not always true for some variables (e.g., E_C, f_D, g_D). Similar to the other global sensitivity analysis methods, MOPSA varies all the parameters simultaneously. The CPDs of acceptable and unacceptable sets for each parameter (e.g., m_R in Fig. 6a) also account for interactions between parameters (Rodrigue-Fernandez et al. 2012), since the acceptable/unacceptable sets are discriminated by the objective function representing the response of a pool to changes in multiple parameters.

Temperature effect on SOC dynamics

The soil C pools could reach a feasible steady state with 3291 out of the 10 000 parameter sets sampled from the parameter distributions/ranges. With an increase of 2°C, the 50% confidence intervals (between the first and third quartiles) of the 100-yr change in C pool size (Fig. 8) indicate (1) the pools of POC-cellulose, MOC, and total SOC increased with dynamic CUE but decreased with constant CUE; (2) the total CO_2 production slightly changed (−0.05 to 0.20%) under dynamic CUE

and increased (0.12 to 0.77%) under constant CUE; (3) both scenarios caused an increase in DOC and decreases in POC-lignin, Q, MBC, and ligninase (EPL); and (4) both cellulase (EPC) and EM decreased under dynamic CUE but cellulase increased and EM remained unchanged under constant CUE. The warming (+2°C) effects considering variations in parameters indicate that the sensitivity of CUE to temperature change had significant effects on all soil C pools except DOC and Q. By excluding the outliers shown in Fig. 8, one might conclude that the changes in SOC pools (POC-lignin, POC-cellulose, MOC, Q) would vary from −8% to 8% under a 2°C increase in temperature.

The typical parameter values in Table 5 were adopted to examine the C pool sizes changing with time. Five scenarios (I–V) of +1 to +5°C were simulated in addition to the baseline run ($T = 12°C$). As aforementioned, CUE and the parameters shown in Table 3 varied with temperature under scenarios I–V. An additional scenario (VI) was conducted with +2°C and constant CUE. The CO_2 efflux (mg C·g soil^{-1}·h^{-1}; Fig. 9a) reached its
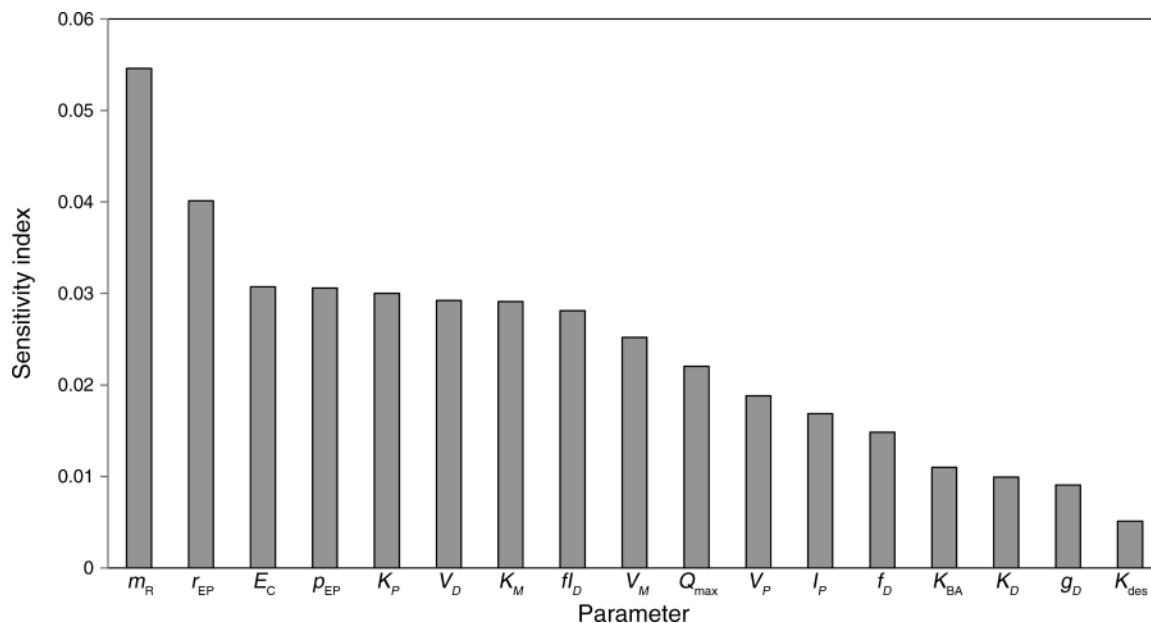
FIG. 7. Overall parameter sensitivity quantified by the sensitivity index with regard to all response variables. Parameters are defined in Table 2.

lowest level during the seventh year under scenarios I–V and resulted in slight decreases of total respiration over 50 years. The CO_2 efflux was higher than the control value during the first 10 years under Scenario VI. Regardless of the scenario, the CO_2 efflux returned to the pre-warming (control) level with very small fluctuations after approximately 10 years, which has been observed in field-based studies (Treseder et al. 2011). After 30 years, the CO_2 efflux completely returned to the control value of 0.16 µg $C·g$ $soil^{-1}·h^{-1}$. This efflux is equivalent to a respiration rate of 1400 g $C·m^{-3}·yr^{-1}$ (bulk density = 1 g C/cm^3) or 350 g $C·m^{-2}·yr^{-1}$ (soil depth = 25 cm), which falls into the observed range of 60–1260 g $C·m^{-2}·yr^{-1}$ (Raich and Schlesinger 1992).

Scenarios I–V predicted a net decrease during the first six years and then a net increase in the total SOC contents (POC-lignin + POC-cellulose + MOC + Q; Fig. 9b). Compared to the equilibrium state, the total SOC pool increased after 50 years with scenarios I–V. On the contrary, scenario VI resulted in a continuous decrease in SOC during the first 10 years (Fig. 9b) and a total loss of 6% of the equilibrium pool size after 50 years.

The response of POC-lignin (Fig. 9c) was much more complex than the other pools. Scenario I caused a slight net increase but Scenario II–V predicted net losses of lignin. Scenarios I–V predicted a net gain of POC-cellulose (Fig. 9d) and MOC (Fig. 9e) and higher temperature resulted in greater accumulation of C in these two pools. Unlike the other pools, which stabilized after 30 years, the pools of POC-lignin and MOC did not return to new near-equilibrium states until 50 years because of their relatively low decomposition rates. The net increases in POC-cellulose and MOC led to net gains

in the total SOC under scenarios I–V. However, scenario VI with constant CUE resulted in a net decrease in the pools of POC-lignin, POC-cellulose, MOC, and Q. The C loss in the Q pool also increased with higher warming temperature (Fig. 9f) under scenarios I–V. Regardless of constant or dynamic CUE with a temperature increase of 2°C, the Q pool became nearly stable with similar C contents after 20 years, although the temporal trends were opposite during the first 20 years. The Q pool decreased under warming conditions because an increase in temperature would increase the rate of desorption relative to adsorption (Conant et al. 2011).

Net increase in DOC was found for each scenario (Fig. 9g). A constant CUE resulted in less DOC uptake and a large increase of DOC in the first few years, and a net increase in DOC overall. In fact, constant CUE produced a net loss over 50 years for the pools of total SOC, POC-lignin, POC-cellulose, MOC, Q, and MBC (see Fig. 9). In contrast, when CUE is allowed to decrease with warming in scenarios I–V, a net loss of DOC was observed for the first few years, followed by a net increase in DOC. Net increase in DOC was observed most likely because desorption was promoted with higher temperature.

Continuous loss of MBC occurred during the first six years under scenarios I–V (Fig. 9h), which was likely the cause of net loss of DOC in the first few years (Fig. 9g). Net loss in MBC increased with higher warming temperature. In addition, dynamic CUE with a small temperature change (+1°C) resulted in more MBC loss than scenario VI with constant CUE. Similar to MBC, net loss of enzyme was found for each enzyme pool under scenarios I–V (Fig. 9i and j; data for EM is not
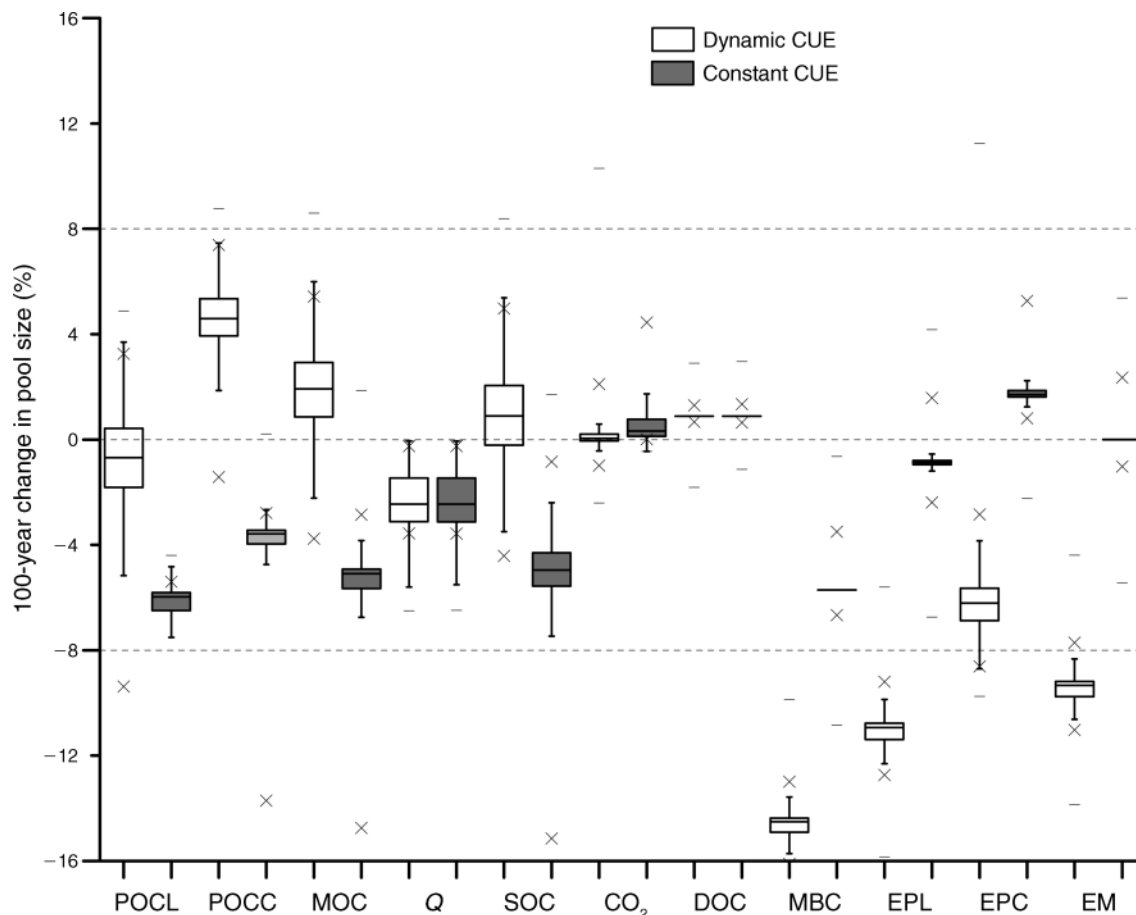
FIG. 8. Boxplots of simulated warming (+2°C) effects on soil C pool sizes over a 100-yr period. Parameter values were sampled from their respective distributions/ranges in Table 5. Dynamic CUE means the carbon use efficiency (CUE) varies with temperature. Const CUE denotes that CUE remains the same as the control treatment (12°C). Soil C pools are POCL, particulate organic carbon-lignin; POCC, particulate organic carbon-cellulose; MOC, mineral-associated organic carbon; Q, adsorbed phase of DOC (dissolved organic carbon); SOC, POCL + POCC + MOC + Q; CO_2, total CO_2 production; MBC, microbial biomass carbon; EPL, EPC, and EM, enzymes for POCL, POCC, and MOC, respectively. The bottom and top of the box denote the 25th and 75th percentile (the lower and upper quartiles), respectively. The band near the middle of the box is the 50th percentile (the median). The ends of the whiskers represent the lowest datum within 1.5 IQR (interquartile range) of the lower quartile, and the highest datum within 1.5 IQR of the upper quartile. The data beyond the two ends of the whiskers might be considered outliers.

shown here). Under scenario VI, however, net increases occurred for all enzyme pools (Fig. 9i and j) during the first 10 years, which corresponded to the increase in MBC (Fig. 9h). The behavior of MBC and enzyme pools was very different for the constant CUE vs. dynamic CUE, which was the most likely cause of the observed different responses in SOC pools. Because dynamic CUE results in lower MBC and enzyme pools, POC-cellulose and MOC tend to accumulate resulting in the overall increase in SOC (Fig. 9b). Constant CUE, in contrast, tends to over-estimate the activities of MBC and enzymes, leading to lower overall SOC. Similar to the constant CUE scenario, however, POC-lignin decreases with dynamic CUE despite observed decreases in ligninase concentration (Fig. 9i). Different behaviors between the POC-lignin and POC-cellulose pools could be interpreted by the changes in individual enzyme pools

and a much higher Ea for the specific lignin degradation rate than for cellulose degradation, which leads to a greater increase in the specific enzyme activity for ligninase than for cellulase under warming conditions. All enzyme pools returned to the baseline sizes after 30 years under scenario VI.

Zhou et al. (2012) found that there is no significant difference in the recalcitrant-C pool between warming (+2°C) and the control for a 10-yr experiment on a tallgrass prairie ecosystem. Our study also indicates the first 10 years as a critical period. The pools of POC-lignin and MOC reached the control values after about 10 years under scenarios I–V (Figs. 9c and e). In particular, POC-lignin decreased in the first three years and then recovered back to the baseline, while very small variations in MOC were observed during the first 10 years.
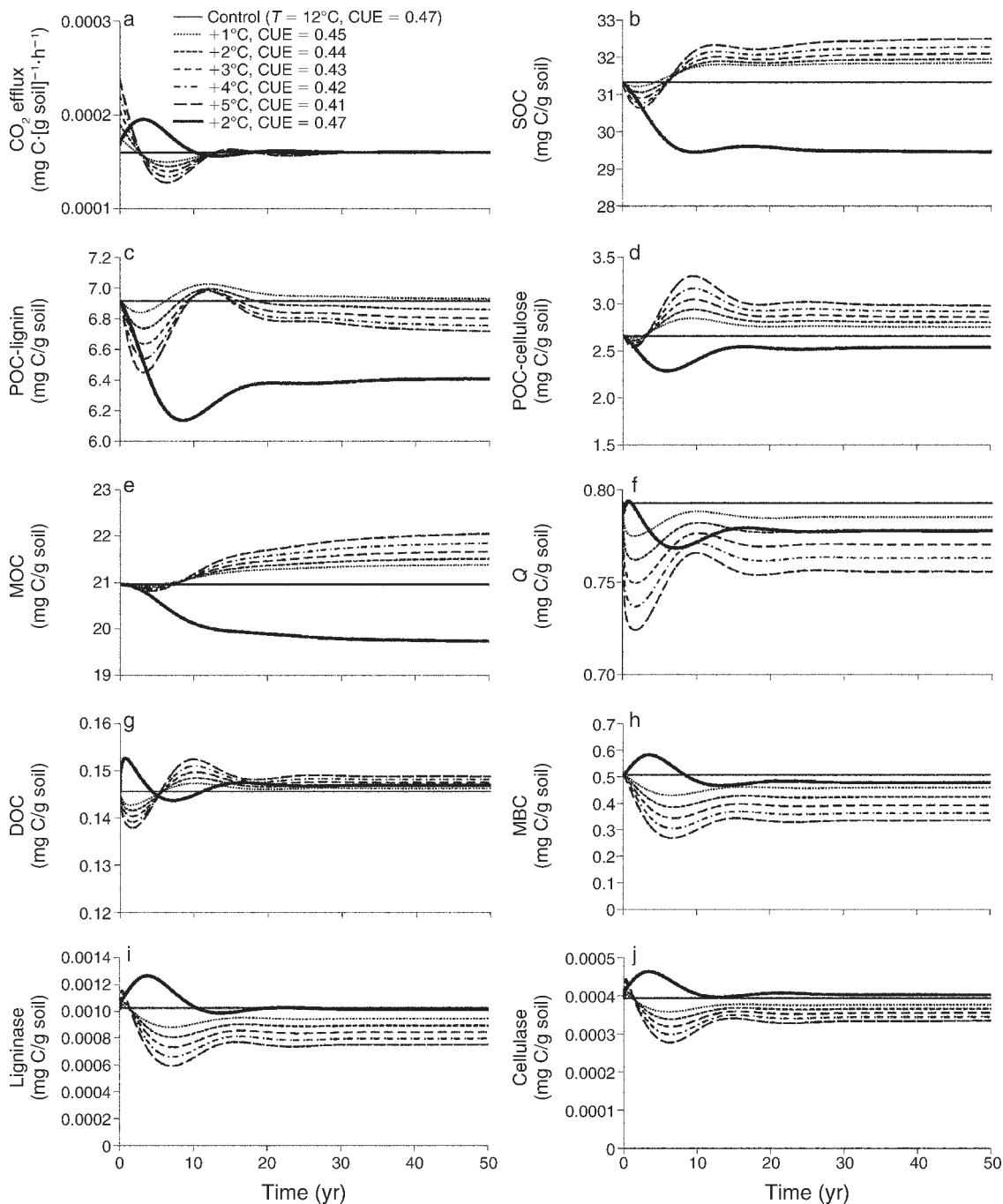
FIG. 9. Simulated warming effects on (a) CO_2 efflux, (b) soil organic carbon ($SOC = POC + MOC + Q$), (c) particulate organic carbon-lignin (POC-lignin), (d) particulate organic carbon-cellulose (POC-cellulose), (e) mineral-associated organic carbon (MOC), (f) adsorbed phase of DOC (Q), (g) dissolved organic carbon (DOC), (h) microbial biomass carbon (MBC), (i) lignin-degrading enzyme (ligninase), and (j) cellulose-degrading enzyme (cellulase). Carbon use efficiency (CUE) was modified by temperature under Scenario I–V but remained the same as the control treatment under Scenario VI ($+2°C$, CUE $= 0.47$). The typical parameter values in Table 5 were adopted and the V_P values ($T = 12°C$ and pH $= 6$) for POC-lignin and POC-cellulose were set to 0.96 and 5.02 mg C·[mg C]$^{-1}$·h^{-1}, respectively.

Although the maximum specific enzyme activities increased under scenario I–V, the decreased MBC led to decreases in enzyme production after several years and then provided negative feedback to decomposition rates.

Take scenario II as an example, the concentrations of ligninase and cellulase were reduced by 21% and 14%, respectively, at around the seventh year, compared to the baseline concentrations (see Figs. 9i and j). Although

the maximum specific enzyme activities of ligninase and cellulase were increased by 17% and 11% due to a temperature increase of 2°C, the maximum enzyme activities (maximum specific enzyme activity multiplied by enzyme concentration) were still reduced by 8% and 4% for ligninase and cellulase, respectively, because of the reductions in enzyme concentration. The enzyme activities were also lower under warming than the control from the seventh to the 11th year, which led to accumulation of C in both POC pools under warming conditions in those years. Thus it is understandable that Zhou et al. (2012) observed that the activity of phenol oxidase remained constant and the activity of peroxidase was significantly lower under warming than the control after 10 years. However, during the first year, the activities of ligninase and cellulase were higher under warming than the control, since both maximum specific enzyme activities and enzyme concentrations were higher. Therefore, the positive response of maximum specific enzyme activity combining positive or negative feedback of enzyme concentration to warming could finally result in increased, unchanged, or reduced enzyme activities, mainly depending on the changing magnitudes of specific enzyme activity and enzyme concentration.

Conclusion

We developed an enzyme-mediated SOC decomposition model with physically measurable pools. Based on the analytical steady-state and dynamic analyses combined with literature estimates, we estimated feasible ranges/distributions for model parameters, such as the maximum specific reaction rates and half-saturation constants for the decompositions of POC and MOC and the uptake of DOC by MBC, the specific maintenance factor and the adsorption and desorption coefficients. The scenario analysis of responses of SOC dynamics to warming indicated that the decreased MBC under warming conditions might lead to decreases in enzyme production and provide negative feedback to decomposition rates. Although the maximum specific enzyme activities increased with increasing temperature, the overall decomposition rates were reduced and the total SOC yielded net accumulation of C over 50–100 yr with regard to warming and dynamic CUE, while a constant CUE might result in a net SOC loss. Our model simulation indicated that SOC losses under warming conditions could occur in the first few years, and subsequently recover because of reductions in decomposition resulting from reductions in microbial biomass and associated enzyme production.

Multiple SOC pools (POC-lignin, POC-cellulose, MOC, and Q) in the MEND model elucidate different responses of various pools to temperature changes and the contributions of various pools to the overall SOC dynamics, which is more informative than the model with a single SOC pool (e.g., Allison et al. 2010). Different behaviors between the POC-lignin and POC-

cellulose pools could be interpreted by the changes in individual enzyme pools and a much higher Ea for the specific lignin degradation rate than for cellulose degradation. The dynamics of different SOC pools reflected the catalytic functions of specific enzymes targeting specific substrates and the interactions between microbes, enzymes, and SOC.

The feasible parameter values and the MOPSA method developed in this study can be used as useful tools to parameterize the decomposition models incorporating microbial-enzyme kinetics. Our current model simplifies the descriptions of enzyme dynamics and the relationships to microbial dynamics. Further steps to incorporate enzyme patterns and responses to substrate chemistry and microbial stoichiometry (Sinsabaugh et al. 2008) into mathematical models will be required for a complete process description.

Literature Cited

Allison, S. D., M. D. Wallenstein, and M. A. Bradford. 2010. Soil-carbon response to warming dependent on microbial physiology. Nature Geoscience 3:336–340.

Aoyama, M., D. A. Angers, and A. N'Dayegamiye. 1999. Particulate and mineral-associated organic matter in water-stable aggregates as affected by mineral fertilizer and manure applications. Canadian Journal of Soil Science 79:295–302.

Chantigny, M. H. 2003. Dissolved and water-extractable organic matter in soils: a review on the influence of land use and management practices. Geoderma 113:357–380.

Choi, J., S. M. Hulseapple, M. H. Conklin, and J. W. Harvey. 1998. Modeling CO_2 degassing and pH in a stream-aquifer system. Journal of Hydrology 209:297–310.

Conant, R. T., et al. 2011. Temperature and soil organic matter decomposition rates—synthesis of current knowledge and a way forward. Global Change Biology 17:3392–3404.

Davidson, E. A., and I. A. Janssens. 2006. Temperature sensitivity of soil carbon decomposition and feedbacks to climate change. Nature 440:165–173.

Davidson, E. A., I. A. Janssens, and Y. Luo. 2006. On the variability of respiration in terrestrial ecosystems: moving beyond Q_{10}. Global Change Biology 12:154–164.

Devevre, O. C., and W. R. Horwath. 2000. Decomposition of rice straw and microbial carbon use efficiency under different soil temperatures and moistures. Soil Biology and Biochemistry 32:1773–1785.

Elshafei, G. S., I. Nasr, A. S. M. Hassan, and S. Mohammad. 2009. Kinetics and thermodynamics of adsorption of cadusafos on soils. Journal of Hazardous Materials 172:1608–1616.

Fröberg, M. J., P. Hanson, P. Swanston, C. Todd, D. Tarver, and C. J. R. Garten. 2007. Low dissolved organic carbon input from fresh litter to deep mineral soils. Soil Science Society of America Journal 71:347–354.

Gjettermann, B., M. Styczen, H. C. B. Hansen, F. P. Vinther, and S. Hansen. 2008. Challenges in modelling dissolved organic matter dynamics in agricultural soil using DAISY. Soil Biology and Biochemistry 40:1506–1518.

Hinz, C. 2001. Description of sorption data with isotherm equations. Geoderma 99:225–243.

Hunt, H. W. 1977. A simulation model for decomposition in grasslands. Ecology 58:469–484.

Jardine, P. M., M. A. Mayes, P. J. Mulholland, P. J. Hanson, J. R. Tarver, R. J. Luxmoore, J. F. McCarthy, and G. V. Wilson. 2006. Vadose zone flow and transport of dissolved organic carbon at multiple scales in humid regimes. Vadose Zone Journal 5:140–152.

Jastrow, J. D. 1996. Soil aggregate formation and the accrual of particulate and mineral-associated organic matter. Soil Biology and Biochemistry 28:665–676.

Jin, Q. S., and C. M. Bethke. 2003. A new rate law describing microbial respiration. Applied and Environmental Microbiology 69:2340–2348.

Kaiser, K., and G. Guggenberger. 2000. The role of DOM sorption to mineral surfaces in the preservation of organic matter in soils. Organic Geochemistry 31:711–725.

Kaiser, K., M. Kaupenjohann, and W. Zech. 2001. Sorption of dissolved organic carbon in soils: effects of soil sample storage, soil-to-solution ratio, and temperature. Geoderma 99:317–328.

Kalbitz, K., S. Solinger, J. H. Park, B. Michalzik, and E. Matzner. 2000. Controls on the dynamics of dissolved organic matter in soils: a review. Soil Science 165:277–304.

Kleber, M., P. Sollins, and R. Sutton. 2007. A conceptual model of organo-mineral interactions in soils: self-assembly of organic molecular fragments into zonal structures on mineral surfaces. Biogeochemistry 85:9–24.

Kothawala, D. N., T. R. Moore, and W. H. Hendershot. 2008. Adsorption of dissolved organic carbon to mineral soils: a comparison of four isotherm approaches. Geoderma 148:43–50.

Kuzyakov, Y., and G. Domanski. 2000. Carbon input by plants into the soil. Review. Journal of Plant Nutrition and Soil Science 163:421–431.

Lawrence, C. R., J. C. Neff, and J. P. Schimel. 2009. Does adding microbial mechanisms of decomposition improve soil organic matter models? A comparison of four models using data from a pulsed rewetting experiment. Soil Biology and Biochemistry 41:1923–1934.

Likas, A., and N. Vlassis. 2003. The global k-means clustering algorithm. Pattern Recognition 36:451–461.

Lilienfein, J., R. G. Qualls, S. M. Uselman, and S. D. Bridgham. 2004. Adsorption of dissolved organic carbon and nitrogen in soils of a weathering chronosequence. Soil Science Society of America Journal 68:292–305.

Mayes, M. A., K. R. Heal, C. C. Brandt, J. R. Phillips, and P. M. Jardine. 2012. Relation between soil order and sorption of dissolved organic carbon in temperate subsoils. Soil Science Society of America Journal 76:1027–1037.

McGuire, K. L., and K. K. Treseder. 2010. Microbial communities and their relevance for ecosystem models: decomposition as a case study. Soil Biology and Biochemistry 42:529–535.

Mehdi, S., M. Halimah, M. Nashriyah, and B. S. Ismail. 2009. Adsorption and desorption of paraquat in two Malaysian agricultural soils. American-Eurasian Journal of Sustainable Agriculture 3:555–560.

Mendham, D. S., E. C. Heagney, M. Corbeels, A. M. O'Connell, T. S. Grove, and R. E. McMurtrie. 2004. Soil particulate organic matter effects on nitrogen availability after afforestation with *Eucalyptus globulus*. Soil Biology and Biochemistry 36:1067–1074.

Michalzik, B., K. Kalbitz, J. H. Park, S. Solinger, and E. Matzner. 2001. Fluxes and concentrations of dissolved organic carbon and nitrogen—a synthesis for temperate forests. Biogeochemistry 52:173–205.

Michalzik, B., E. Tipping, J. Mulder, J. F. G. Lancho, E. Matzner, C. L. Bryant, N. Clarke, S. Lofts, and M. A. V. Esteban. 2003. Modelling the production and transport of dissolved organic carbon in forest soils. Biogeochemistry 66:241–264.

Moorhead, D. L., and R. L. Sinsabaugh. 2006. A theoretical model of litter decay and microbial interaction. Ecological Monographs 76:151–174.

Mrabet, R., N. Saber, A. El-Brahli, S. Lahlou, and F. Bessam. 2001. Total, particulate organic matter and structural stability of a Calcixeroll soil under different wheat rotations and tillage systems in a semiarid area of Morocco. Soil and Tillage Research 57:225–235.

Neff, J. C., and G. P. Asner. 2001. Dissolved organic carbon in terrestrial ecosystems: Synthesis and a model. Ecosystems 4:29–48.

NOAA. 2011. National (Contiguous U.S.) Temperature 1895–2008. National Oceanic and Atmospheric Administration, National Climatic Data Center, Asheville, North Carolina, USA. http://www.noaanews.noaa.gov/stories2009/images/1208natltemp.png

Novak, J. M., P. M. Bertsch, and G. L. Mills. 1992. Carbon-13 nuclear magnetic resonance spectra of soil water-soluble organic carbon. Journal of Environmental Quality 21:537–539.

Ott, L., and M. Longnecker. 2010. An introduction to statistical methods and data analysis. Sixth edition. Duxbury Press, Belmont, California, USA.

Park, S., and N. Agmon. 2008. Theory and simulation of diffusion-controlled Michaelis-Menten kinetics for a static enzyme in solution. Journal of Physical Chemistry B 112:5977–5987.

Pirt, S. J. 1965. Maintenance energy of bacteria in growing cultures. Proceedings of the Royal Society B 163:224–231.

Post, W. M., W. R. Emanuel, P. J. Zinke, and A. G. Stangenberger. 1982. Soil carbon pools and world life zones. Nature 298:156–159.

Qualls, R. G. 2000. Comparison of the behavior of soluble organic and inorganic nutrients in forest soils. Forest Ecology and Management 138:29–50.

R Development Core Team. 2011. R: a language and environment for statistical computing. R Foundation for Statistical Computing, Vienna, Austria. www.r-project.org

Raich, J. W., and W. H. Schlesinger. 1992. The global carbon dioxide flux in soil respiration and its relationship to vegetation and climate. Tellus B 44:81–99.

Rodrigue-Fernandez, M., J. R. Banga, and F. J. Doyle III. 2012. Novel global sensitivity analysis methodology accounting for the crucial role of the distribution of input parameters: application to systems biology models. International Journal of Robust and Nonlinear Control 22:1082–1102.

Rudzinski, W., and T. Panczyk. 2000. Kinetics of isothermal adsorption on energetically heterogeneous solid surfaces: a new theoretical description based on the statistical rate theory of interfacial transport. Journal of Physical Chemistry B 104:9149–9162.

Schimel, J. P., and M. N. Weintraub. 2003. The implications of exoenzyme activity on microbial carbon and nitrogen limitation in soil: a theoretical model. Soil Biology and Biochemistry 35:549–563.

Schlesinger, W. H., and J. Lichter. 2001. Limited carbon storage in soil and litter of experimental forest plots under increased atmospheric CO_2. Nature 411:466–469.

Schmidt, M. W. I., M. S. Torn, S. Abiven, T. Dittmar, G. Guggenberger, I. A. Janssens, M. Kleber, I. Kögel-Knabner, J. Lehmann, and D. A. C. Manning. 2011. Persistence of soil organic matter as an ecosystem property. Nature 478:49–56.

Sinsabaugh, R. L., et al. 2008. Stoichiometry of soil enzyme activity at global scale. Ecology Letters 11:1252–1264.

Six, J., G. Guggenberger, K. Paustian, L. Haumaier, E. T. Elliott, and W. Zech. 2001. Sources and composition of soil organic matter fractions between and within soil aggregates. European Journal of Soil Science 52:607–618.

Sohn, S., and D. Kim. 2005. Modification of Langmuir isotherm in solution systems—definition and utilization of concentration dependent factor. Chemosphere 58:115–123.

Tabatabai, M. A. 2003. Soil enzymes. Pages 1451–1462 *in* J. R. Plimmer, D. W. Gammon, and N. N. Ragsdale, editors. Encyclopedia of agrochemicals. John Wiley, Hoboken, New Jersey, USA.

Treseder, K. K., T. C. Balser, M. A. Bradford, E. L. Brodie, E. A. Dubinsky, V. T. Eviner, K. S. Hofmockel, J. T. Lennon, U. Y. Levine, and B. J. MacGregor. 2011. Integrating microbial ecology into ecosystem models: challenges and priorities. Biogeochemistry 1–12.

van Bodegom, P. 2007. Microbial maintenance: a critical review on its quantification. Microbial Ecology 53:513–523.

Vandenbruwane, J., S. De Neve, R. G. Qualls, S. Sleutel, and G. Hofman. 2007. Comparison of different isotherm models for dissolved organic carbon (DOC) and nitrogen (DON) sorption to mineral soil. Geoderma 139:144–153.

Van de Werf, H., and W. Verstraete. 1987. Estimation of active soil microbial biomass by mathematical analysis of respiration curves: calibration of the test procedure. Soil Biology and Biochemistry 19:261–265.

Van Griensven, A., T. Meixner, S. Grunwald, T. Bishop, M. Diluzio, and R. Srinivasan. 2006. A global sensitivity analysis tool for the parameters of multi-variable catchment models. Journal of Hydrology 324:10–23.

van Iersel, M. W., and L. Seymour. 2000. Growth respiration, maintenance respiration, and carbon fixation of vinca: a time series analysis. Journal of the American Society for Horticultural Science 125:702–706.

van Iersel, M., and L. Seymour. 2002. Temperature effects on photosynthesis, growth respiration, and maintenance respiration of marigold. Pages 549–554 *in* T. Blom and R. Criley. XXVI International Horticultural Congress—elegant sciences in floriculture. Canadian International Development Agency (CIDA), Gatineau, Quebec, Canada.

Wang, G., and S. Chen. 2012. A review on parameterization and uncertainty in modeling greenhouse gas emissions from soil. Geoderma 170:206–216.

Wang, G., S. Chen, and C. Frear. 2012*a*. Estimating greenhouse gas emissions from soil following liquid manure applications using a unit response curve method. Geoderma 170:295–304.

Wang, G., and W. M. Post. 2012. A theoretical reassessment of microbial maintenance and implications for microbial ecology modeling. FEMS Microbiology Ecology 81:610–617.

Wang, G., W. M. Post, M. A. Mayes, J. T. Frerichs, and S. Jagadamma. 2012*b*. Parameter estimation for models of ligninolytic and cellulolytic enzyme kinetics. Soil Biology and Biochemistry 48:28–38.

Wang, G., and J. Xia. 2010. Improvement of SWAT2000 modelling to assess the impact of dams and sluices on streamflow in the Huai River basin of China. Hydrological Processes 24:1455–1471.

Wang, G., J. Xia, and J. Chen. 2009. Quantification of effects of climate variations and human activities on runoff by a monthly water balance model: A case study of the Chaobai River basin in northern China. Water Resources Research 45:W00A11.

Yurova, A., A. Sirin, I. Buffam, K. Bishop, and H. Laudon. 2008. Modeling the dissolved organic carbon output from a boreal mire using the convection-dispersion equation: Importance of representing sorption. Water Resources Research 44:W07411.

Zhou, J., K. Xue, J. Xie, Y. Deng, L. Wu, X. Cheng, S. Fei, S. Deng, Z. He, J. D. Van Nostrand, and Y. Luo. 2012. Microbial mediation of carbon-cycle feedbacks to climate warming. Nature Climate Change 2:106–110.

SUPPLEMENTAL MATERIAL

Supplement

Full data for soil organic carbon (SOC), dissolved organic carbon (DOC), and microbial biomass carbon (MBC) collected from the literature (*Ecological Archives* A023-015-S1).